Pergamon

Tetrahedron: *Asymmetry* 11 (2000) 53–73

TETRAHEDRON: *ASYMMETRY*

The design, synthesis and biological evaluation of neuraminic acid-based probes of *Vibrio cholerae* sialidase

Jennifer C. Wilson, Robin J. Thomson, Jeffrey C. Dyason, Pas Florio, Kaylene J. Quelch, Samia Abo and Mark von Itzstein *

Department of Medicinal Chemistry, Monash University (Parkville Campus), 381 Royal Parade, Parkville, Victoria 3052, Australia

Received 9 November 1999; accepted 2 December 1999

Abstract

A molecular modelling study using the program GRID has been used to investigate the structural requirements of a potential inhibitor binding to *Vibrio cholerae* sialidase. A number of favourable interactions were predicted between the sialidase and Neu2en derivatives containing hydroxyl- or halogen-substituted acyl groups on the C-5 amine. As a result of this study, a detailed analysis of the interactions of C-5-substituted Neu2en derivatives with the active site of *V. cholerae* sialidase was undertaken using a conformational searching routine based on molecular dynamics. Based on the results of these molecular design studies several *N*-acyl-Neu2en-based probes were prepared and evaluated for sialidase inhibition. As envisaged, and pleasingly, the designed compounds were found to be accommodated by the enzyme's active site architecture, and to be strong inhibitors of *V. cholerae* sialidase.

1. Introduction

The significant biological roles played by sialic acids (e.g. *N*-acetylneuraminic acid, Neu5Ac **1**) in normal physiological processes, and also in disease states and microbial infection, has led to the widespread study of the proteins that recognize this class of compounds.[1–4] Knowledge of the three-dimensional structure of a sialic acid-recognizing protein through an X-ray crystal structure can lead to a greater understanding of protein–substrate/inhibitor interactions and aid in the design of potential inhibitors. The X-ray crystal structures of a number of sialic acid-recognizing proteins, both metabolizing enzymes, e.g. *N*-acetylneuraminate lyase[5] and several sialidases,[6–21] as well as adhesion proteins such as influenza virus haemagglutinin[22] and E-selectin,[23] have been solved. In the case of sialidases from strains of influenza virus, analyses of X-ray crystal structures have shown that a number of amino

* Corresponding author. Fax: +61-3-9903-9672; e-mail: mark.vonitzstein@vcp.monash.edu.au

0957-4166/00/$ - see front matter
PII: S0957-4166(99)00552-2

acids that line and surround the walls of the active site pocket are invariant in all strains of the virus characterized so far.[8] This finding led to the rational design,[24,25] using molecular modelling techniques such as described herein, and development of the potent and selective inhibitor of the sialidase, 5-acetamido-2,6-anhydro-3,4,5-trideoxy-4-guanidino-D-*glycero*-D-*galacto*-non-2-enoic acid **2**.[25–31] The 4-deoxy-4-guanidino-Neu5Ac2en derivative **2** has subsequently been developed as the *anti*-influenza drug Zanamivir (Relenza®).[29–31]

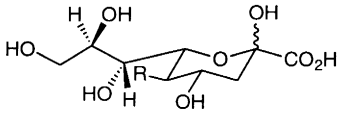

1 Neu5Ac; R = NHAc

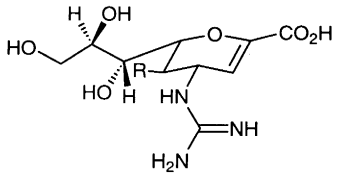

2 R = NHAc

Sialic acid-recognizing proteins such as the sialidases from pathogenic organisms are obvious targets for the design of potential therapeutic agents.[6,8,29] The sialidase associated with the bacterium *Vibrio cholerae* is believed to have two roles in cholera disease. Firstly, *V. cholerae* sialidase is part of a multi-enzyme mucinase complex,[32] which may function in the pathogenesis of the bacterium by reducing the viscosity of the gastrointestinal mucus, thereby facilitating access of the bacterium to the target epithelial cells. Secondly, as depicted in Fig. 1, *V. cholerae* sialidase cleaves sialic acids from higher order gangliosides to give GM_1, the putative cholera toxin receptor.[33,34] It therefore appears that the sialidase may increase the virulence of *V. cholerae* by increasing the number of receptor sites available for binding of cholera toxin.

A number of structure–activity studies have been carried out on *V. cholerae* sialidase.[27,35–45] These studies have included the use of modified sialic acid glycosides as potential substrates,[35–37,41,45] and 2,3-unsaturated sialic acid derivatives[27,37–39,43,44] based on 5-acetamido-2,6-anhydro-3,5-dideoxy-D-*glycero*-D-*galacto*-non-2-enoic acid (*N*-acetyl-Neu2en, Neu5Ac2en, **3**), as well as non-carbohydrate compounds,[36,42] as potential inhibitors. Neu5Ac2en **3** itself is a μM inhibitor of the enzyme.[27] It is postulated to be a transition-state analogue,[14,46] based on its half-chair conformation,[47] mimicking the putative sialosyl cation intermediate[14,48,49] **4** in the proposed mechanism of sialidase catalysis.

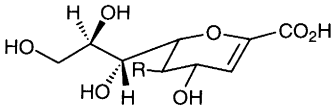

3 Neu5Ac2en; R = NHAc

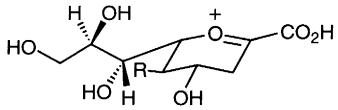

4 R = NHAc

In 1994, the X-ray structure of *V. cholerae* sialidase solved to 2.3 Å was published[17] allowing a closer examination of the enzyme active site and comparison[17] with the sialidases from influenza virus[8] and *Salmonella typhimurium*.[15] As shown in Fig. 2 the sialidase from *V. cholerae* consists of a central catalytic domain that is associated with two lectin domains.

Described herein is an investigation of the active site of *V. cholerae* sialidase using molecular modelling techniques. In particular, we have examined the area of the active site that accommodates the C-5 acetamido group of Neu5Ac. Based on the results of this study, a number of C-5-modified derivatives of Neu5Ac2en **3** have been synthesized and evaluated as inhibitors of the sialidase. Furthermore, we have taken the opportunity to interpret previously reported inhibition data[38,39,43,44] in light of our conclusions drawn from the present molecular modelling study.

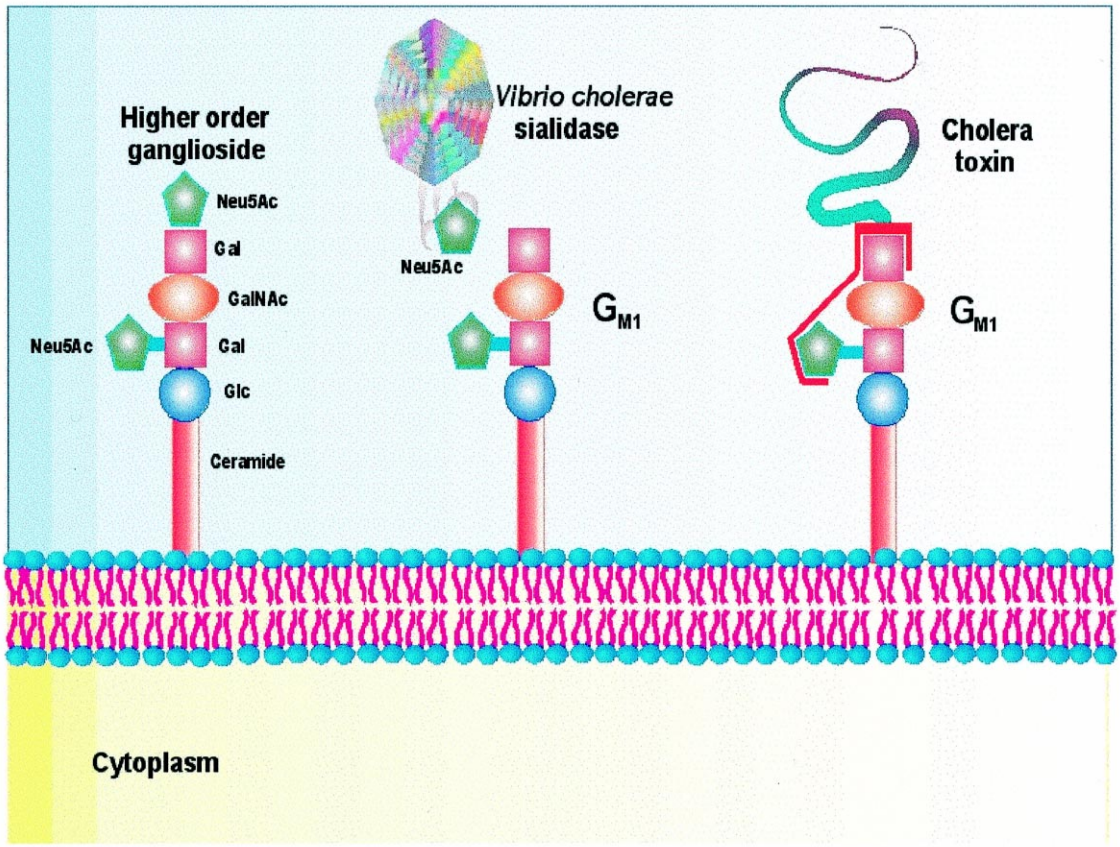

Fig. 1. Cleavage of a higher-order ganglioside by *Vibrio cholerae* sialidase to give GM_1, the putative receptor for cholera toxin

2. Results and discussion

2.1. Molecular modelling

The overall topology of the *V. cholerae* active site cavity, in which Neu5Ac2en[17] or Neu5Ac bind with the β-face of the pyranose ring towards the floor of the cavity, can be described as a pocket with a deep cavity directly below the C-4-*epi* position which extends underneath, around to the C-5 position as shown in Fig. 3. The upper surface of the pocket is formed by Asp250 that sits directly above the C-4 position, Asn318 which sits above the C-5 acetamido group, and hydrophobic residues Phe638 and Leu580 which encase the C-8/C-9 position.

The *V. cholerae* sialidase active site contains an array of residues that are conserved among the bacterial sialidases from *S. typhimurium*[15] and *Micromonospora viridifaciens*,[18] the sialidases from different strains of influenza virus,[8–14] and the intramolecular '*trans*-sialidase' from the leech (*Macrobdella decora*),[19] for which X-ray crystal structures have been solved. The conserved array of residues in *V. cholerae* sialidase, which have been detailed by Crennell et al. (summarised in Table 1),[17] are those that are potentially involved in the enzyme catalytic mechanism. However, there are some differences between the sialidases in other areas of the active site, in particular in the vicinity of C-4 and of the C-6 glycerol side chain of Neu5Ac.[17–19] In each of the sialidases crystallized to date,[8,15,17–19] there is a hydrophobic pocket which accommodates the C-5 acetamido substituent of Neu5Ac. In *V. cholerae* sialidase, this

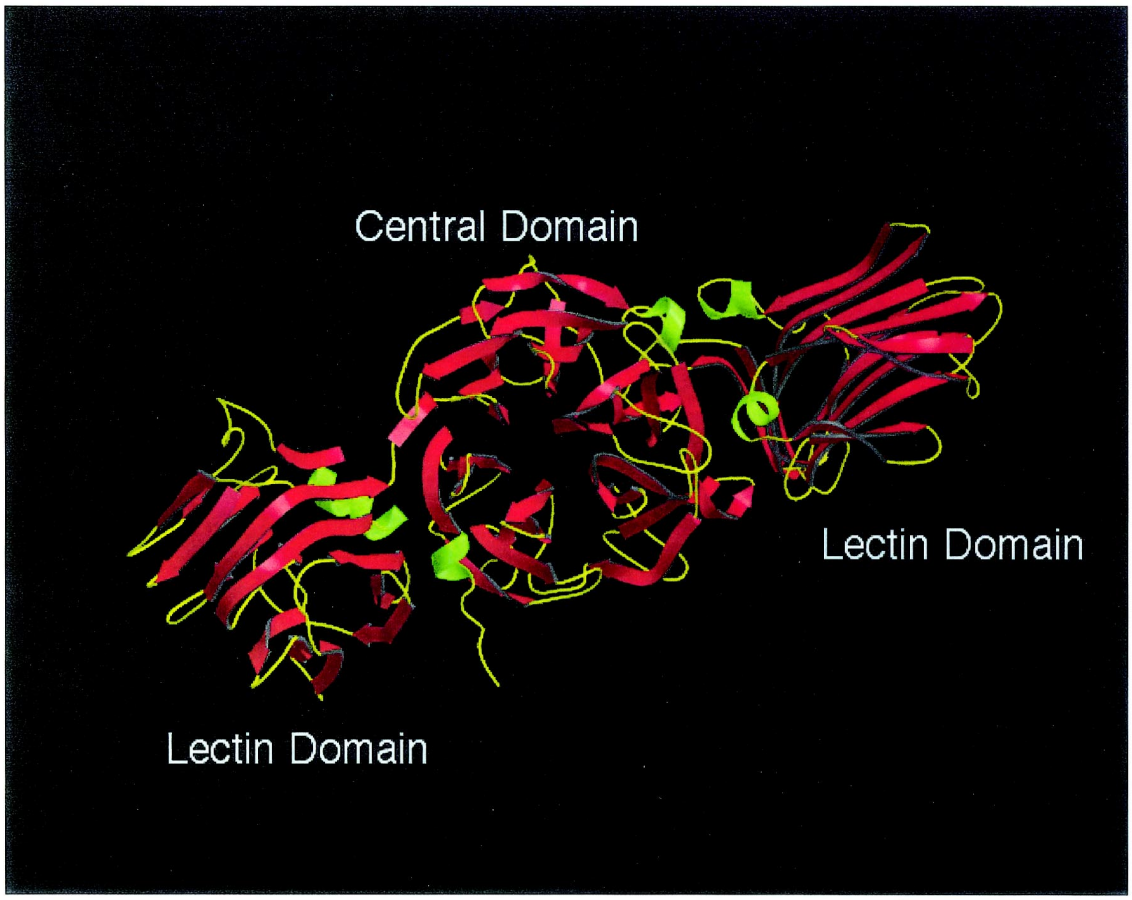

Fig. 2. Structure of *Vibrio cholerae* sialidase. The central domain is the sialidase function and is flanked by lectin domains

pocket is relatively large, with quite extensive cavities adjacent to and below the C-5 acetamido group. In a general inspection of the C-5 binding domain we concluded that an interaction between the active site residue Asn318 and the C-5 acylamino carbonyl is possible. This observation supports the view[35,41,44,45] that this carbonyl group may be required for recognition by *V. cholerae* sialidase.

Fig. 4 shows some of the interactions between the active site residues of *V. cholerae* sialidase and Neu5Ac2en **3**. Similar active site interactions are observed for Neu5Ac **1**.

2.1.1. GRID calculations

The program GRID[50] was used to investigate the active site of *V. cholerae* sialidase. GRID is a molecular design tool that can be used to investigate the steric and electronic interactions between functional group probes and biomolecules. Contour maps are calculated to identify regions of favourable interaction energy between the functional group probes and the biomolecule. In these calculations only contributions within a 35 Å cube centred on the catalytically important residues were considered. A range of functional group probes were investigated for this study and, as detailed below, several of these have provided useful information. The areas of favourable interaction energy noted were examined with α-*N*-acetylneuraminic acid (2-α-Neu5Ac) modelled in the active site. Contour maps showing the most

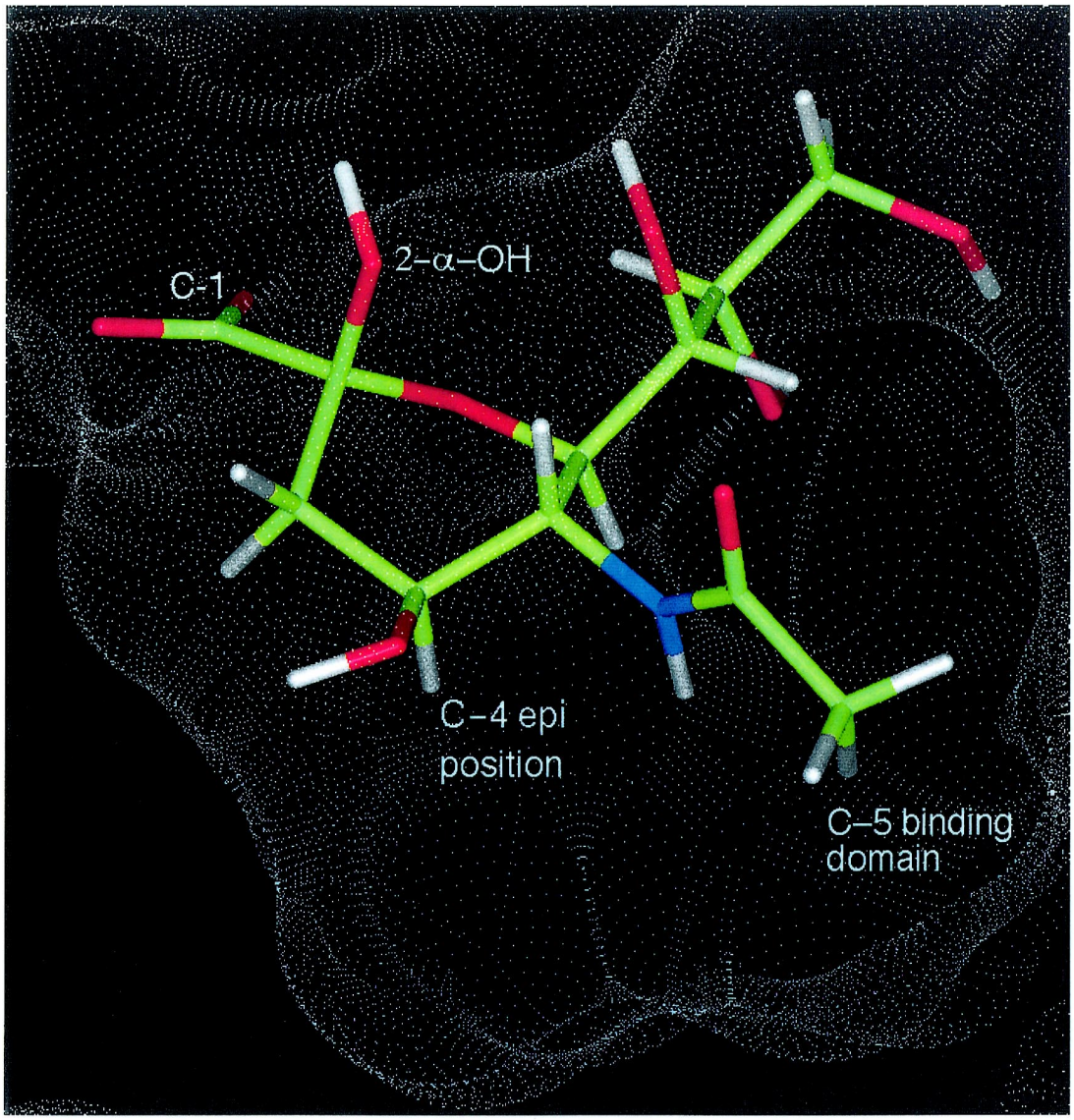

Fig. 3. A view of 2-α-Neu5Ac modelled in the active site of *Vibrio cholerae* sialidase

favourable interactions for carboxyl, hydroxyl, chloro, amino, and methyl probes, with 2-α-Neu5Ac positioned in the active site, are presented in Figs. 5–9, respectively.

2.1.1.1. Carboxyl group probe. The carboxyl group probe (Fig. 5) showed a region of favourable interaction energy (in magenta) at -7 kcal mol^{-1} that accurately predicted the positioning of the Neu5Ac C-2 carboxylate located in a cluster of three arginine residues (224, 635 and 712) within the active site.

These arginine residues form strong interactions with the acid group on Neu5Ac, as determined from binding energy calculations, and therefore have a role in holding the Neu5Ac residue in place during the catalytic process.[49] GRID analysis revealed no other positions of favourable interaction for a carboxylate group within the active site. Other similar probes such as phosphate, sulfone, and nitro groups were also predicted to bind well within the triarginyl cluster. However, from the point of view of inhibitor design,

Table 1
The important conserved residues in the active site of *Vibrio cholerae* sialidase[17]

Residue:	Comments:
Arg224, 635, 712	The arginine residues stabilize the carboxylate group of Neu5Ac [a]
Tyr740	This tyrosine is believed to be important in stabilizing the sialosyl cation intermediate formed during the enzymic hydrolysis of sialyl glycosides [b]
Glu756	Glu756 stabilizes Arg224 [c]
Asp250	Asp250 may act as a proton donor to the glycosidic oxygen at low pH or be involved in stabilizing a proton-donating H_2O molecule [d]

[a] Refs 15,49; [b] Refs 14,15; [c] Ref 15; [d] Refs 14,48

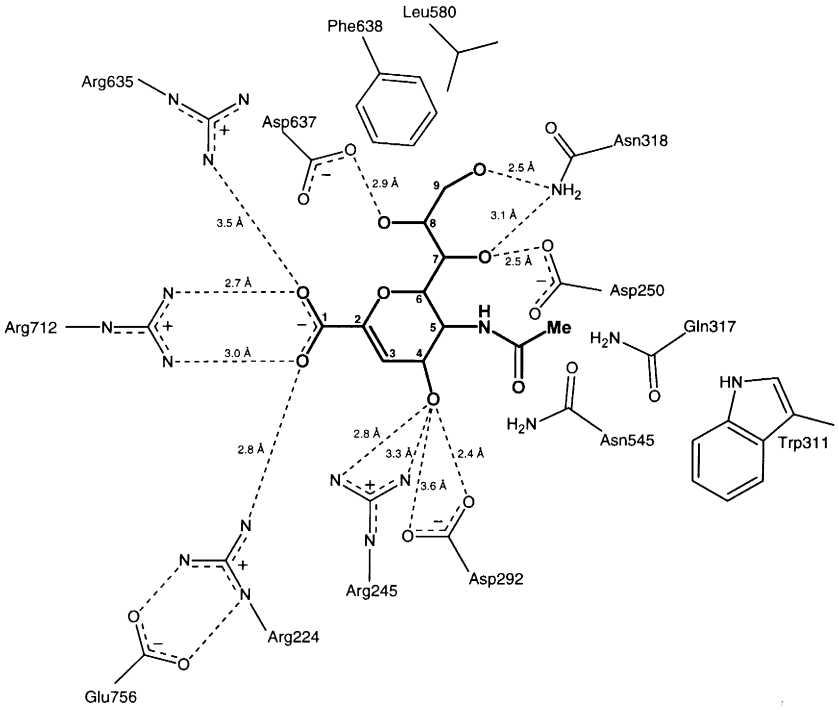

Fig. 4. Important interactions between the active site residues of *Vibrio cholerae* sialidase and Neu5Ac2en **3**

substitution of these groups on the sialic acid framework at C-2, in preference to a carboxylate group, is not expected to be advantageous. Indeed, the phosphonic acid analogue of Neu5Ac2en,[51] showed a slight reduction in inhibition of *V. cholerae* sialidase compared to Neu5Ac2en.[52] Crystal structures determined with 2-deoxy-phosphonic acid analogues of Neu5Ac bound to *S. typhimurium*[16] and influenza virus[21] sialidases showed that interaction between the phosphonyl group and the triarginyl cluster was a major contributing factor in the determination of the inhibitor binding mode.[16,21]

2.1.1.2. Hydroxyl group probe. The hydroxyl group probe (Fig. 6) showed at -11 kcal mol^{-1} regions of favourable interaction energy (in blue) corresponding to the location of the carboxylate group on Neu5Ac. At the same contour level 'hot-spots' were also seen located near the methyl of the C-5

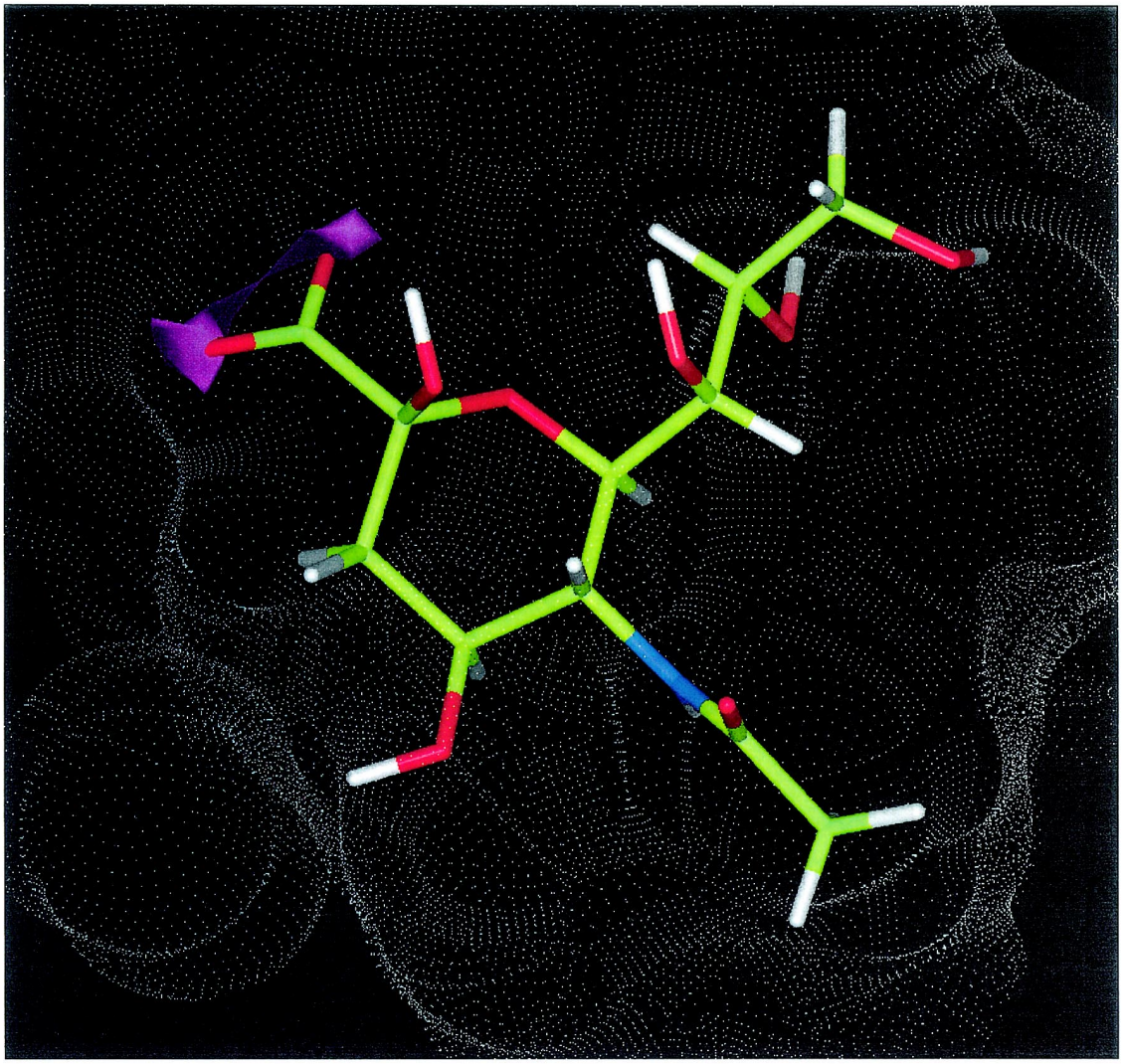

Fig. 5. Contour map showing the most favourable interactions (in magenta) at −7 kcal mol^{-1} for the carboxyl group probe with 2-α-Neu5Ac modelled in the active site

acetamido group that as previously mentioned resides in quite a deep pocket of the active site. This led us to the conclusion that the *N*-glycolyl [NHC(O)CH_2OH] derivative of neuraminic acid should be accommodated well in that region of the active site.

Additionally, at −7 kcal mol^{-1}, regions of contours (not shown) were seen extending from the C-3 position on Neu5Ac to the position of the C-4 hydroxyl group. In this region of the active site are situated Arg245 (2.8/3.3 Å) and Asp292 (2.4/3.6 Å) which would be expected to interact with the C-4 hydroxyl group, contributing to these favourable contour energies. Similar 'pairs' of arginine and aspartate residues are observed to interact with the C-4 hydroxyl group in the sialidases from *S. typhimurium*,[15] *M. viridifaciens*,[18] and the intramolecular *trans*-sialidase from leech.[19] In influenza virus sialidase, however, there do not appear to be extensive interactions with the C-4 hydroxyl group,[16] which is accommodated in a large cavity.[8]

Examination of the interactions of the hydroxyl group probe in the glycerol side chain binding region

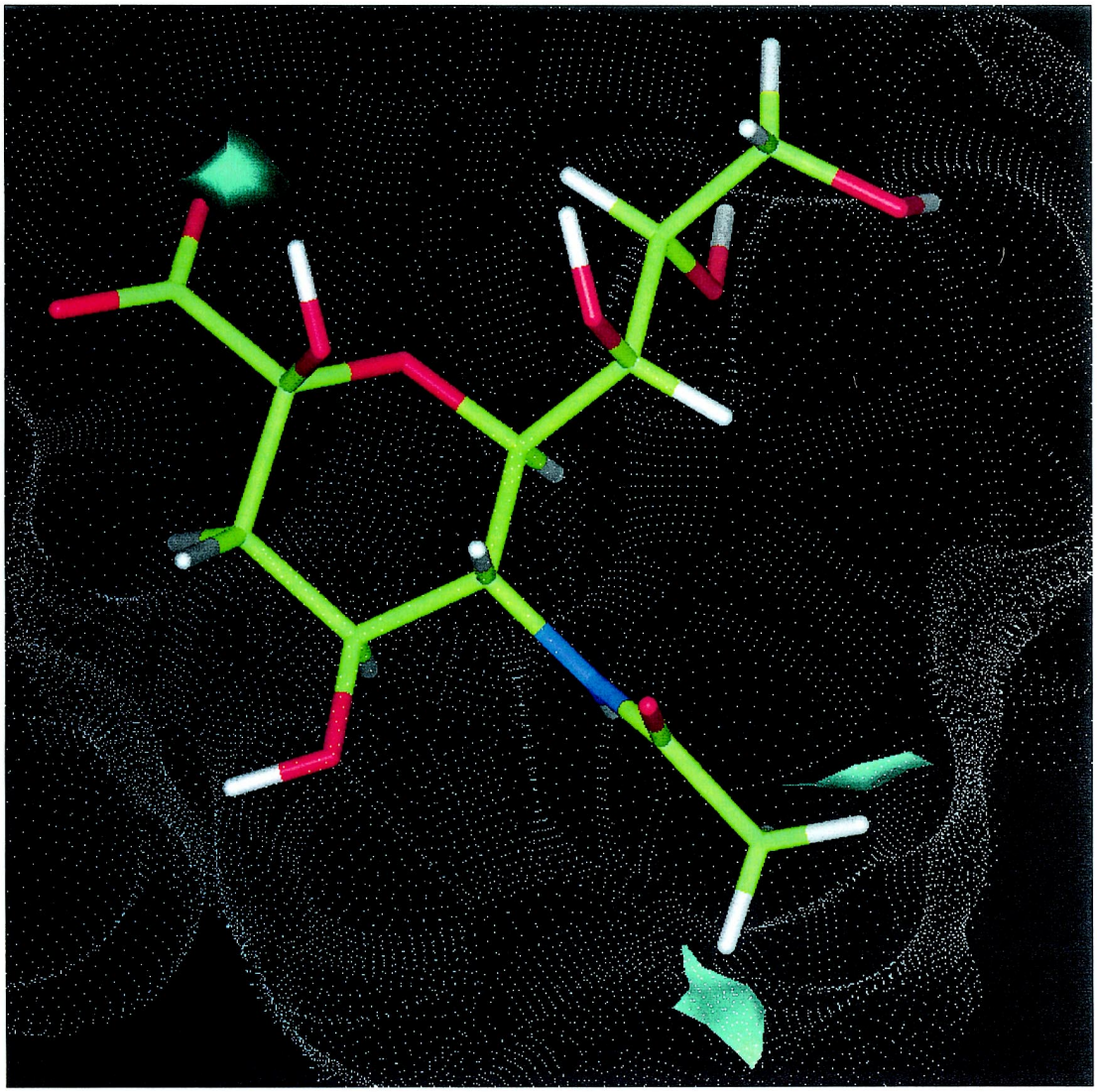

Fig. 6. Contour map showing the most favourable interactions (in blue) at -11 kcal mol^{-1} for the hydroxyl group probe with 2-α-Neu5Ac modelled in the active site

revealed contours (not shown), at -6 kcal mol^{-1}, located near the C-7 hydroxyl and C-8 hydroxyl groups of Neu5Ac. In this region of the active site, Asn318 could interact with the C-7 hydroxyl group (3.1 Å) and C-9 hydroxyl group (2.5 Å). In addition, Asp637 form a hydrogen bond with the C-8 hydroxyl group (2.9 Å). The C-7 hydroxyl group could also participate in a hydrogen bonding interaction with solvent exposed Asp250 (2.5 Å).

2.1.1.3. Halogen probes. The chloro (Fig. 7) and fluoro probes showed several areas of favourable interaction. The chloro probe had contours (in yellow) at -4 kcal mol^{-1} extending from the C-3 position on Neu5Ac to, and below, the C-4 position. Favourable contours were also located in the vicinity of the methyl of the C-5 acetamido group.

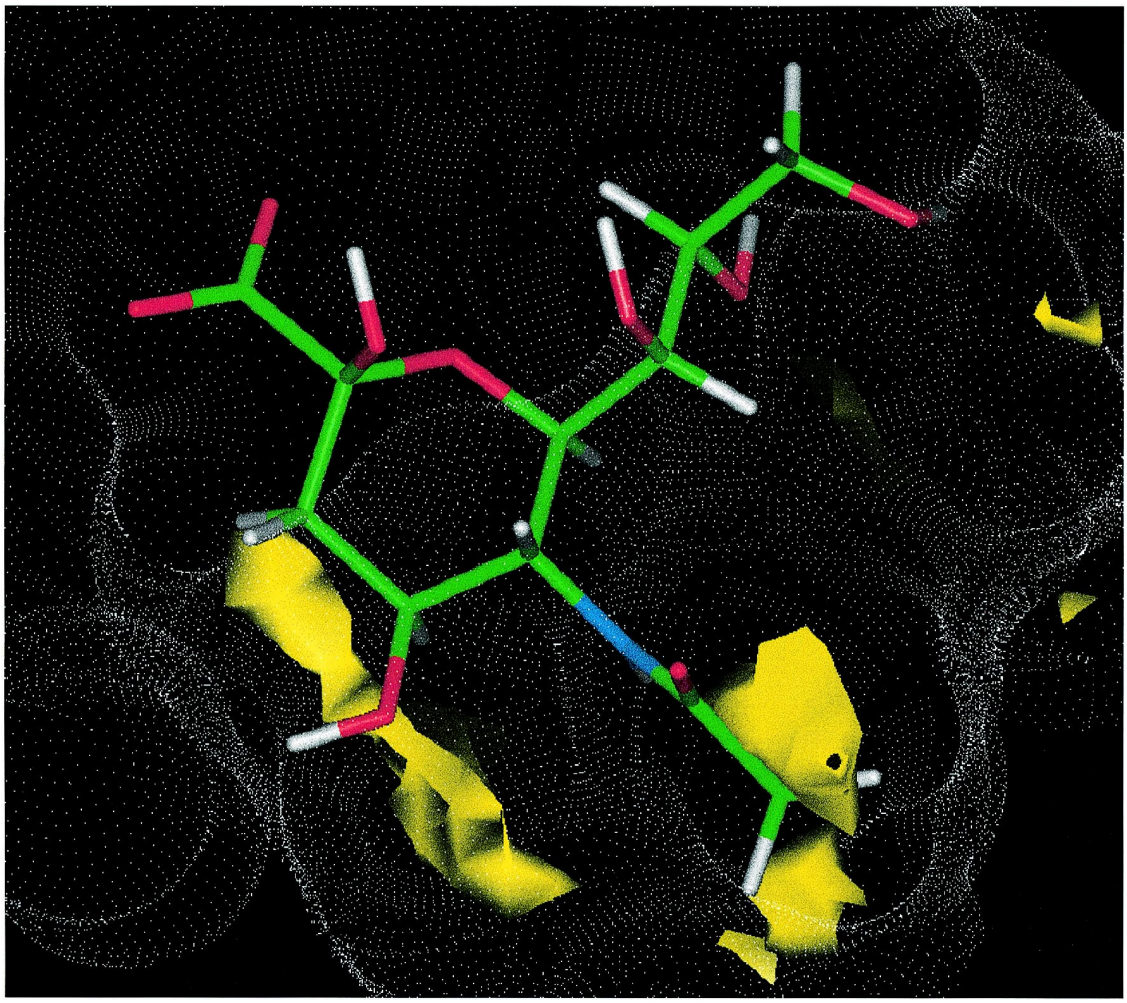

Fig. 7. Contour map showing the most favourable interactions (in yellow) at −4 kcal mol^{-1} for the chloro probe with 2-α-Neu5Ac modelled in the active site

Interestingly, no favourable contours were seen for the bromo or iodo probes in the C-5 pocket. The most likely explanation for this result is that both bromine and iodine atoms are too bulky to be accommodated in this region of the active site.

2.1.1.4. Nitrogen-based probes. In general the nitrogen-based probes (e.g. amino group probe, Fig. 8) gave the best interaction energies with contours (in blue) being distinguishable at −18 kcal mol^{-1}. Close examination of these contours revealed that they were in regions below the *epi*-position at the C-4 position of Neu5Ac, in the vicinity of the acidic residues Glu243, Glu619 and Asp292. At higher interaction energies (−9 kcal mol^{-1}, not shown) contours were located near the methyl of the C-5 acetamido group within the active site.

It is noteworthy that no favourable contours were seen around the equatorial position at C-4 of Neu5Ac. A similar GRID study of influenza virus sialidase[24] identified favourable interactions for a nitrogen probe in a large cavity found around the equatorial C-4 position. This led to the synthesis[26] of

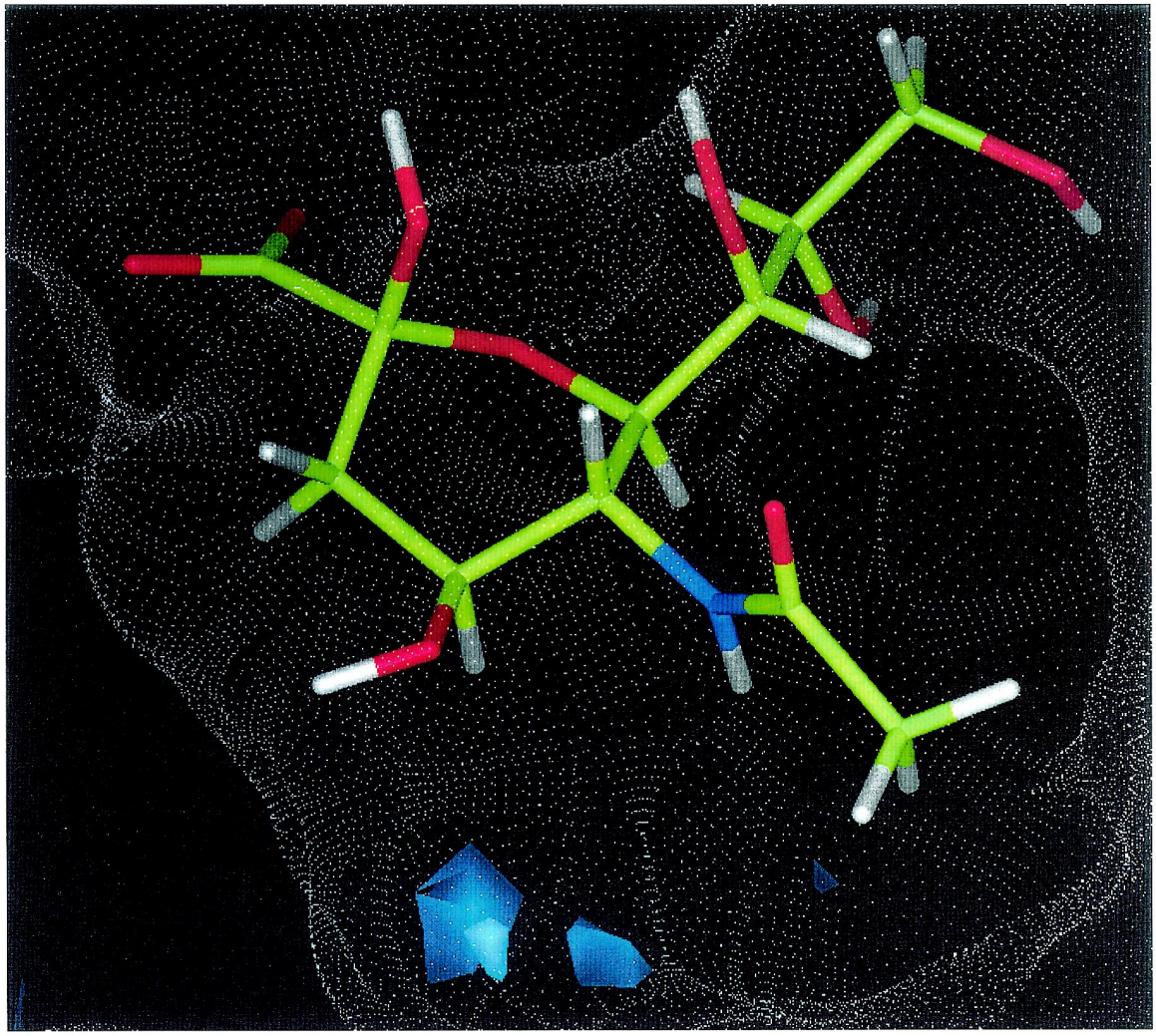

Fig. 8. Contour map showing the most favourable interactions (in blue) at −18 kcal mol^{-1} for the amino group probe with 2-α-Neu5Ac modelled in the active site

Neu5Ac2en derivatives containing amino and guanidino groups at C-4, for example **2**, which interacted with acidic active site residues located in this region,[12,25] and that proved to be potent and selective inhibitors of influenza virus sialidase.[25,27,29] Analysis of the crystal structures of the bacterial sialidases from *V. cholerae*[17] and *S. typhimurium*[15] shows that there is no similar cavity at C-4 and that a guanidino group would be too sterically demanding to be able to fit in this position. This observation, which was predicted,[27] but unconfirmed until the crystal structure analysis of *V. cholerae* sialidase was completed, explains why 4-deoxy-4-guanidino-Neu5Ac2en (Zanamivir, Relenza®) was found to exhibit far less inhibition of the bacterial sialidases than of influenza virus sialidase.[27]

2.1.1.5. Aliphatic/aromatic based probes. Hydrophobic probes such as methyl (Fig. 9), methylene and phenyl were investigated and in general were contoured at much higher interaction energies (e.g. −3 kcal mol^{-1}). Clearly from Fig. 9 it can be seen that there are significant regions of favourable interaction

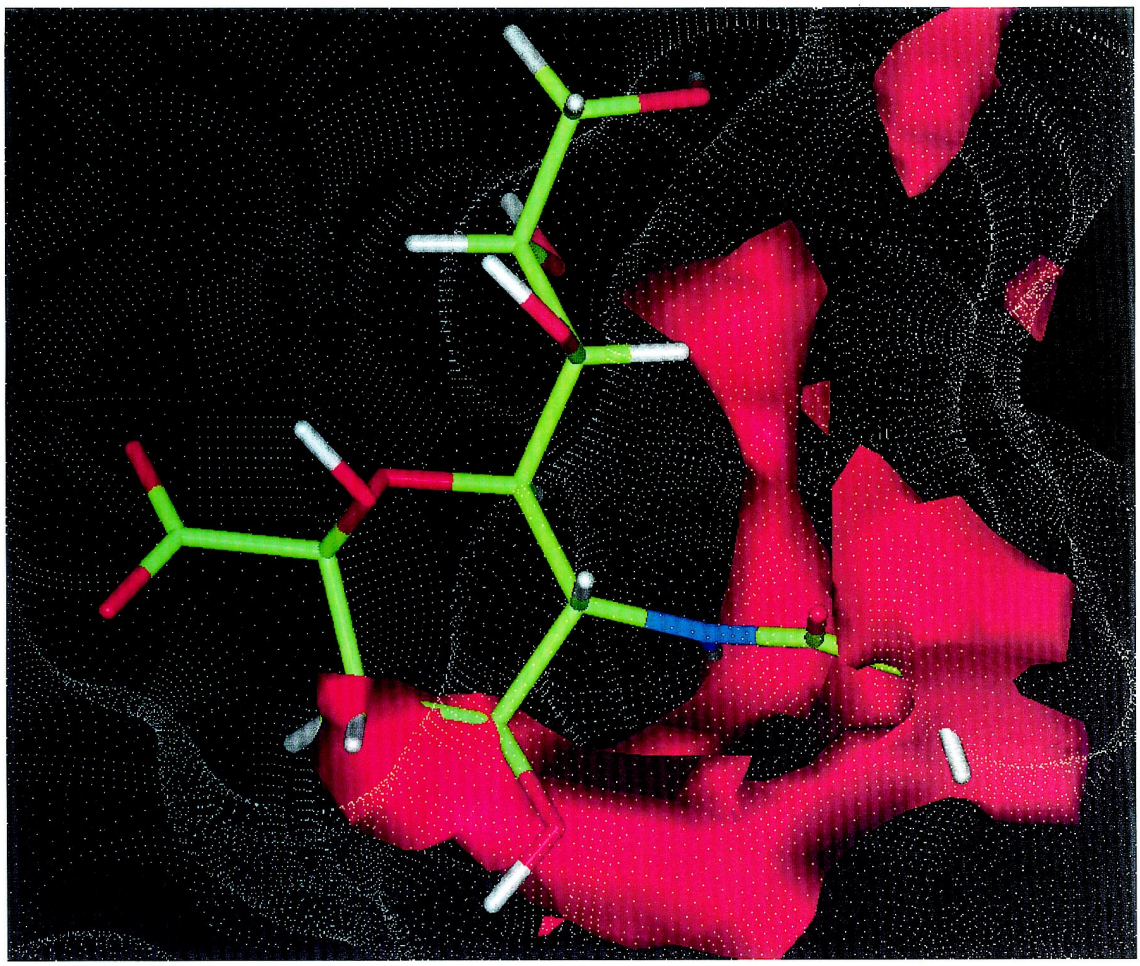

Fig. 9. Contour map showing the most favourable interactions (in red) at −3 kcal mol^{-1} for the methyl group probe with 2-α-Neu5Ac modelled in the active site

energies (in red) corresponding to the positioning of the methyl of the C-5 acetamido group as well as around the C-3 methylene of 2-α-Neu5Ac.

In the cavity around C-5 there is a conserved tryptophan residue (also found in *S. typhimurium*[15] and influenza virus[8] sialidases) which, in the case of influenza virus sialidase, makes important hydrophobic contacts (4.0 Å) to the methyl of the C-5 acetamido group of Neu5Ac.[11] Mutation of this residue in influenza virus sialidase led to a properly expressed, transported and folded protein which, however, retained no sialidase activity.[53] In *V. cholerae* sialidase, this conserved Trp311 is situated ca. 4.1 Å from the methyl of the C-5 acetamido group of Neu5Ac.

2.1.2. Conformational searching routines for C-5-modified Neu5Ac2en derivatives

The GRID analysis of the active site cavity of *V. cholerae* sialidase showed that there were possibilities for investigating modifications to the C-5 acetamido group and substitution at the C-4-*epi* position with a view to improving the binding of potential inhibitors of the sialidase. To further investigate the influence that modifications to the C-5 acetamido group would have on binding, a series of C-5-modified Neu5Ac2en derivatives were examined in the active site of *V. cholerae* sialidase. Neu5Ac2en **3** was

chosen as the starting template for the molecular modelling protocol as it is, as previously mentioned, a μM inhibitor of *V. cholerae* sialidase.[27]

C-5-Modified Neu5Ac2en derivatives were built-up, situated in the active site of the fully minimized *V. cholerae* sialidase structure and then subjected to a conformational searching protocol based on molecular dynamics calculations. These calculations were performed to identify potential binding modes of the modified Neu5Ac2en derivatives within the active site pocket. Choice of the modification at C-5 was guided to some extent by the aforementioned GRID studies. Although many different functional group possibilities were examined in the GRID study only those that showed interesting interactions with the active site will be discussed here.

2.1.2.1. N-*Glycolyl-Neu2en* ***5***. The *N*-glycolyl derivative interacts with several residues in the vicinity of the C-5 binding domain of the active site cavity. Specifically, hydrogen bonding interactions (3.4 Å) were seen between the amide carbonyl of Gln317 and the hydroxyl group of the *N*-glycolyl moiety. Some conformers from the searching routine were also seen with interactions between the *N*-glycolyl hydroxyl group and Asp292 at 2.9 Å and Asn545 at 3.1 Å.

2.1.2.2. N-*Chloroacetyl-Neu2en* ***6***. Chain extension of the *N*-acetyl by a chlorine atom seemed to have little overall impact on the binding of the analogue compared to the Neu5Ac2en starting template. Initially, it was anticipated that the chlorine would form a hydrogen bond to the amine groups of the asparagine residues that sit above and below the methyl of the C-5 acetamido group. The conformational searching routine results do not support this however, and it seems more likely that the chlorine interacts with the hydrophobic Trp311 situated 3.8 Å away.

*2.1.2.3. Aliphatic chain extensions [*N-*propanoyl-* ***7****,* N-*butanoyl-* ***8****, and* N-*(acryloyl)-* ***9*** *Neu2en].* The effects of aliphatic, one and two carbon, chain extensions to the *N*-acetyl group were also investigated by the conformational searching protocol. The conformational search revealed that the C-5 binding domain of the active site could accommodate an *N*-propanoyl or *N*-acryloyl side chain but chain extension to the *N*-butanoyl group was not accommodated. Similarly, replacing the methyl of the *N*-acetyl with a phenyl ring giving *N*-benzoyl-Neu2en was also not possible on steric grounds. These results indicated that there was little scope for improving inhibition through chain extension, even though adjacent to and below the C-5 acetamido group there is quite an extensive cavity. The C-5 binding domain of the active site is able to accommodate differences in flexibility with the *N*-propanoyl and *N*-acryloyl groups being accommodated equally well. The *N*-acryloyl derivative participates in hydrophobic interactions with Trp311 (3.3. Å) and Pro251 (3.7 Å) in the C-5 binding domain.

2.2. Synthesis of C-5-modified Neu5Ac2en derivatives

The data from the molecular modelling studies supported the notion that *N*-glycolyl-Neu2en **5** and *N*-chloroacetyl-Neu2en **6** should be accommodated by the enzyme's active site, and in particular the C-5 substituents, *N*-glycolyl and *N*-chloroacetyl, may be able to access favourable interactions with a number of active site residues. These interactions could potentially result in improved inhibition of the sialidase when compared with the benchmark compound Neu5Ac2en. The inhibition of *V. cholerae* sialidase by both of these compounds has previously been reported by others,[39,43] although in each case different assays were used to evaluate sialidase inhibition making it difficult to compare the data. As a result of these differences we decided to re-investigate these compounds so that we could obtain

a direct comparison of inhibition between them and Neu5Ac2en in a fluorescence assay procedure. Furthermore, and as explained in the molecular modelling section, we concluded that the active site architecture around the C-5 binding domain should be able to accommodate some hydrophobic electron rich functionalities such as an acryloyl group. The preparation of the *N*-acryloyl derivative **9** was achieved from the reactive intermediate *N*-(3-chloropropanoyl)-Neu2en. In addition and for completeness, *N*-trichloroacetyl-Neu2en **10** was synthesised to observe the effects of introducing a very bulky and electronically demanding group.

The procedure used for the preparation of the C-5-modified Neu5Ac2en derivatives is outlined in Scheme 1.

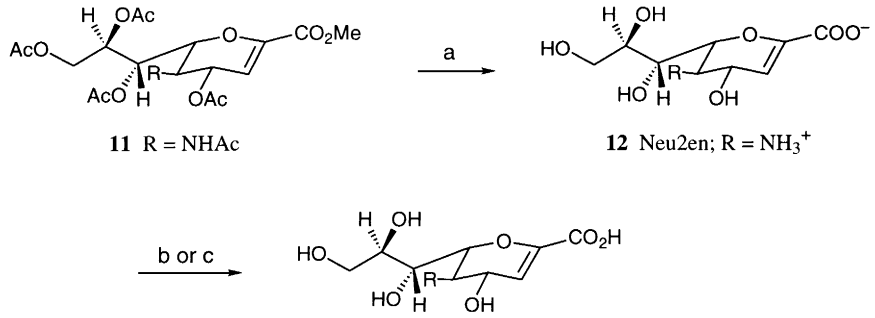

11 R = NHAc

12 Neu2en; R = NH_3^+

5 *N*-glycolyl-Neu2en; R = $NHCOCH_2OH$

6 *N*-chloroacetyl-Neu2en; R = $NHCOCH_2Cl$

9 *N*-acryloyl-Neu2en; R = $NHCOCH{=}CH_2$

10 *N*-trichloroacetyl-Neu2en; R = $NHCOCCl_3$

Scheme 1. *Reagents and conditions*: (a) $Ba(OH)_2$, H_2O, 90°C; (b) (i) Et_3N, THF, H_2O, rt; (ii) R′COOH, DCC, rt; (c) Et_3N, MeOH, R′COCl, −60°C

Methyl 5-acetamido-4,7,8,9-tetra-*O*-acetyl-2,6-anhydro-3,5-dideoxy-D-*glycero*-D-*galacto*-non-2-enoate[54] **11** was deprotected and de-*N*-acetylated by reaction with aqueous barium hydroxide[55] at ca. 90°C for several hours to give an 85% yield of Neu2en **12**. This yield is similar to the 89% yield reported by Isecke and Brossmer for the de-*N*-acetylation of the fully protected 2-α-methyl ketoside of Neu5Ac with barium hydroxide.[55] *N*-Acylation of Neu2en,[44,56,57] and neuraminic acid derivatives,[55,58–62] with a variety of agents has been previously reported. In this work the reaction was carried out by means of either a dicyclohexylcarbodiimide (DCC)-mediated coupling with a carboxylic acid, or by reaction with an acid chloride.

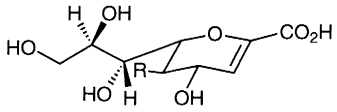

7 *N*-propanoyl-Neu2en; R = $NHCOCH_2CH_3$

8 *N*-butanoyl-Neu2en; R = $NHCOCH_2CH_2CH_3$

13 *N*-trifluoroacetyl-Neu2en; R = $NHCOCF_3$

14 *N*-iodoacetyl-Neu2en; R = $NHCOCH_2I$

15 *N*-formyl-Neu2en; R = NHCOH

2.3. Inhibition of Vibrio cholerae *sialidase*

Using a well known fluorometric assay,[27] inhibition constants (K_i values) were determined for the C-5-modified Neu5Ac2en derivatives synthesised, as well as Neu5Ac2en itself, and these data are presented in Table 2. The inhibition constants for both *N*-glycolyl-Neu2en[43] **5** and *N*-chloroacetyl-Neu2en[39] **6**, relative to Neu5Ac2en, are comparable with those found in previously reported inhibition studies as further elaborated in the following discussion. Furthermore, we have taken the opportunity to now

Table 2
Inhibition data against *Vibrio cholerae* sialidase for Neu5Ac2en and C-5-modified derivatives of Neu5Ac2en

Compound	K_i (μM)
N-acetyl-Neu2en (Neu5Ac2en, **3**)	3.56
N-glycolyl-Neu2en (Neu5Gc2en, **5**)	2.61
N-chloroacetyl-Neu2en (**6**)	3.45
N-trichloroacetyl-Neu2en (**10**)	250
N-acryloyl-Neu2en (**9**)	2.55

interpret, at the molecular level, some of the biological data[38,39,43,44] that has been reported in the past for a range of C-5-modified Neu5Ac2en derivatives.

2.3.1. N-*Glycolyl-Neu2en*

The GRID study had indicated contours for favourable interactions of the hydroxyl group probe in the vicinity of the methyl of the C-5 acetamido group of Neu5Ac. The molecular dynamics investigation of the unsaturated *N*-glycolyl derivative **5** indicated conformers with hydrogen bonding interactions between the glycolyl hydroxyl group and several residues in the active site. The inhibition data obtained here, and previously (Nöhle et al.[43] reported IC_{50} values against *V. cholerae* sialidase of 1.0×10^{-5} M for Neu5Gc2en **5**, and 1.5×10^{-5} M for Neu5Ac2en **3**), is supportive of the proposal that the *N*-glycolyl group improves binding into the active site compared to the *N*-acetyl group.

2.3.2. N-*Haloacetyl-Neu2en derivatives*

The most potent sialic acid-based inhibitor of *V. cholerae* sialidase reported to date is the *N*-trifluoroacetyl-Neu2en derivative **13**,[39,44] with a 10-fold increase in inhibition over Neu5Ac2en. In addition, both the *N*-monofluoroacetyl- and *N*-difluoroacetyl-Neu5Ac2en derivatives show improved inhibitory activity over Neu5Ac2en.[39] Inhibition data (IC_{50}) determined for *N*-haloacetyl-Neu2en derivatives against *V. cholerae* sialidase by Meindl et al.[39] is presented in Table 3. The GRID study tallies with these findings, with a fluoro probe showing favourable interactions in the vicinity of the methyl of the C-5 acetamido group of Neu5Ac. No evidence of hydrogen-bonding interactions that could contribute to this increased inhibition was observed in the molecular dynamics calculations and therefore the likely increase in inhibition may result from interaction with the hydrophobic residues of the C-5 binding domain.

Table 3
Inhibition data against *Vibrio cholerae* sialidase for Neu5Ac2en and *N*-haloacetyl-Neu2en derivatives; *N*-C(O)R-Neu2en[39]

R	CH_3 (**3**)	CH_2Cl (**6**)	CH_2F	CHF_2	CF_3 (**13**)	CH_2I (**14**)
IC_{50} (10^{-5} M)	3.0	1.0	0.95	0.32	0.25	8.0

The GRID results with the chloro probe led us to conclude that a chloroacetyl group should be accommodated in the C-5 binding domain and moreover participate in favourable interactions with amino acid residues in this domain. However, in the molecular dynamics investigation no apparent improvement

of interactions of the *N*-chloroacetyl analogue **6**, when compared with Neu5Ac2en, was found. It is interesting to note that the molecular dynamics findings are indeed reflected in the comparable inhibition constants (Table 2) for **6** and Neu5Ac2en **3**.

The larger iodo probe showed no favourable interaction energies in the area of the C-5 pocket, presumably due to steric restrictions. In agreement with this observation, the *N*-iodoacetyl-Neu2en derivative **14** was reported[39] to produce a slightly weaker inhibition when compared to Neu5Ac2en. Predictably, therefore, based on steric bulk and electronic demands, substitution of the *N*-acetyl group by an *N*-trichloroacetyl group leads to a dramatic (~100-fold) loss of inhibition (Table 2).

2.3.3. Effects of altering the aliphatic chain of the N-*acyl group*

The GRID study and conformational searching routines indicated that extension of the *N*-acetyl side chain by one carbon to give the *N*-propanoyl or *N*-acryloyl derivatives could be accommodated, but further aliphatic extension or introduction of a phenyl group could not. The molecular dynamics investigation also suggested that chain extensions by one carbon from the parent *N*-acetyl group may actually be favourable, taking advantage of hydrophobic interactions with Trp311. Indeed the *N*-acryloyl derivative **9** produced a slight improvement in inhibition (Table 2). Likewise, Meindl et al.[38] reported a similar trend in inhibition results with an increase in inhibition by the *N*-propanoyl derivative **7** relative to Neu5Ac2en (Table 4), but found that increasing the length of the acyl chain beyond propanoyl led to a reduction in the inhibition of *V. cholerae* sialidase. It is not clear at this stage if unsaturation in the acyl chain improves the level of inhibition because it is difficult to compare absolute inhibition constants across the two assays. However, it is not unreasonable to speculate that the alkenyl moiety may participate in some π–π interactions with Trp311.

Table 4
Inhibition data against *Vibrio cholerae* sialidase for Neu5Ac2en and C-5-modified derivatives with different acyl-group chain lengths; *N*-C(O)R-Neu2en[38]

R	CH_3 (**3**)	CH_2CH_3 (**7**)	$CH_2CH_2CH_3$ (**8**)	Ph
K_i (10^{-5} M)	1.0	1.6	36	3000

Other work by Meindl and Tuppy demonstrated that the replacement of the *N*-acetyl group by *N*-formyl resulted in an approximately 30-fold drop in inhibition of the sialidase (IC_{50} values: 8.0×10^{-4} M for *N*-formyl-Neu2en **15**, vs 3.0×10^{-5} M for Neu5Ac2en **3**).[39] We believe that this finding can be rationalized from the present molecular modelling study. It is not unreasonable to suggest that the loss of the methyl group would lead to a concomitant decrease in the hydrophobic interaction with Trp311 and therefore result in poorer binding affinity.

3. Summary

Although there is a large cavity in the active site pocket of *V. cholerae* sialidase around the C-5 position, and a large number of amino acids available to participate in electrostatic interactions, generally only marginal increases in inhibition over *N*-acetyl-Neu2en have been achieved by substitutions at C-5 to date. The small improvement in inhibition seen with the *N*-glycolyl substituent could be accounted for as being due to potential interaction with several active site residues. The slight increases in inhibition observed for *N*-haloacetyl-, *N*-propanoyl- and *N*-acryloyl-Neu2en derivatives appear to stem from interaction with the hydrophobic areas of the side chain pocket.

The major constraint on which groups will be tolerated in the C-5 pocket appears to be steric. The cavity in the active site leading away from the C-5 position, allows for extension of the *N*-acetyl group by one carbon, or other atom, but a longer aliphatic chain or a more sterically demanding group is not accommodated.

In conclusion, we have investigated the active site architecture of *V. cholerae* sialidase using the previously determined crystal structure[17] and GRID software. From these results we have designed and synthesized a number of neuraminic acid-based probes that appear to be well accommodated by the active site. These results provide important information regarding the active site pocket of *V. cholerae* sialidase that may facilitate the further design and synthesis of potent inhibitors of this enzyme.

4. Experimental

Professor Garry Taylor (St. Andrews University) kindly provided the crystal structure coordinates of *V. cholerae* sialidase at 2.3 Å resolution.

4.1. Molecular modelling

GRID calculations: Calculations were carried out on silicon graphics R8000 and R4000 workstations using GRID version 11.[50] The results and the crystal structures were viewed using InsightII (MSI, San Diego, CA). GRID calculations were performed on a cube of 35 Å per side, centred on the active site, with a GRID spacing of 0.5 Å. The interaction energy between the probe and every atom within the protein structure was evaluated at each grid point. A dielectric constant of 80 was used to simulate a bulk aqueous phase, while areas as determined by GRID to be excluded from solvent were assigned a dielectric constant of 4 (e.g. the interior of the protein). The utility program GRIN was used to automatically assign atom types and charges for the protein using the standard parameter file provided with GRID. The output was converted (using GINI, supplied with GRID) into a suitable form for input into the MSI utility Contour. Contour maps were built-up using steps of 2 kcal mol^{-1}. The contour map was then viewed superimposed on the crystal structure of the active site of *V. cholerae* sialidase using the program InsightII. The GRID results were conveniently displayed using contour maps of the interaction energies superimposed on the crystal structure of the sialidase, together with a solvent accessible surface overlaid on a 15 Å radius of the active site residues and *N*-acetylneuraminic acid (Neu5Ac) positioned in the binding pocket.

Binding of C-5-modified Neu5Ac2en derivatives: The method used to calculate binding modes of the C-5-modified Neu5Ac2en derivatives has been described in detail by Taylor and von Itzstein.[49,63] Firstly, a complete minimization of the *V. cholerae* sialidase crystal structure with Neu5Ac bound, crystallographic waters and a 15 Å cap of solvent water over the active site was performed. The effects of hydration were modelled by partially solvating the active site of the complex and by using a distance dependent dielectric. The minimization was carried out within Discover (MSI) using the Consistent Valence Force Field with a cut-off distance of 15 Å. A multistep protocol was used to ensure the minimization of the strained interactions arising from the crystal structure refinement. First, solvent water molecules were energy minimized with all other atoms fixed, and then all protein backbone and Neu5Ac non-hydrogen atoms were included in the minimization process, followed by the protein side chains, and finally the entire system was free to move. Calculations were done using the algorithms steepest descents (in all constrained minimizations for up to 500 iterations) and conjugate gradients (down to a maximum atomic root mean square derivative of 0.01 kcal mol^{-1}).

Conformational space of the enzyme–ligand complex within the active site was explored using a combination of constrained molecular dynamics and molecular mechanics calculations. Beginning with the energy minimized sialidase/Neu5Ac complex a ligand (previously built-up using InsightII) was docked into the active site with its position and conformation as similar to Neu5Ac as possible. Solvent molecules were then added or subtracted from the area around the docked ligand depending on the space requirements. The complex was constrained throughout all calculations; only the ligand and protein residues within a 15 Å radius of the active site (centred on the C-2 position of sialic acid) and the water molecules around the active site (crystallographic and soak water) were free to move. In addition to the atom constraints, solvent molecules within the active site were subjected to harmonic restraints, with a force constant of 0.05 kcal mol^{-1}, to accurately model solvent mobility. An initial energy minimization was performed to relieve steric strain associated with the newly docked ligand. Molecular dynamics calculations were then performed at 350 K using the leapfrog algorithm in Discover. Dynamics were equilibrated for 2 ps with time steps of 1 fs and then continued for 2 ps with time steps of 2 fs. The resulting structure was extracted and energy minimized. A further 2 ps of dynamics with a time step of 2 fs were performed, with the final structure being again subjected to energy minimization. This protocol was performed 15 times beginning at the molecular dynamics initialization stage.

4.2. Syntheses

General: ^{1}H and ^{13}C NMR spectra were recorded in D_2O using a Bruker AM-300 spectrometer. Chemical shifts are given in ppm relative to external Me_4Si. ESI mass spectra were obtained using a Micromass Platform II electrospray spectrometer, and HRMS were obtained using a Bruker BioApex II FTMS. Optical rotations were measured using a Jasco DIP-370 digital polarimeter. Reactions were monitored by TLC on aluminium plates coated with silica gel 60 F_{254} (Merck). Amines were visualized with ninhydrin. Dowex 50WX8 (400, H^+ form) and Dowex 1X8 (400, Cl^- form) ion exchange resins were washed and activated before use. Methyl 5-acetamido-4,7,8,9-tetra-*O*-acetyl-2,6-anhydro-3,5-dideoxy-D-*glycero*-D-*galacto*-non-2-enoate **11**[54] was prepared in-house. 2-Acetoxyacetic acid was prepared by acetylation of glycolic acid (Aldrich) with acetyl chloride and was recrystallized from toluene (mp 66–68.5°C, lit.[64] 66–68°C). Chloroacetic acid (Koch-Light) was recrystallized from benzene. Dicyclohexylcarbodiimide (DCC) (Fluka), trichloroacetyl chloride (Aldrich) and 3-chloropropionyl chloride (Fluka) were distilled before use.

4.2.1. 5-Amino-2,6-anhydro-3,5-dideoxy-D-glycero-D-galacto-*non-2-enoic acid Neu2en **12***

A suspension of methyl 5-acetamido-4,7,8,9-tetra-*O*-acetyl-2,6-anhydro-3,5-dideoxy-D-*glycero*-D-*galacto*-non-2-enoate **11** (657 mg, 1.39 mmol) in saturated aqueous barium hydroxide[55] (30 ml) was heated at ca. 90°C for 18 h. TLC (15:4:0.5 *i*PrOH:H_2O:AcOH); Neu5Ac2en **3** R_f 0.41, Neu2en **12** (ninhydrin $^+$ve) R_f 0.25. The reaction was cooled, filtered through a Celite plug, and the brown residue was washed thoroughly with water. The filtrate was neutralized by the addition of small pieces of solid carbon dioxide, with vigorous stirring, and then the fine precipitate of $BaCO_3$ was filtered-off and washed thoroughly with water. The precipitate was resuspended in water and stirred for a further 10 min before refiltration. This procedure was repeated three times. The combined filtrates were treated with portions of Dowex 50WX8 (H^+) resin (ca. 10 ml total) until the supernatant tested negative for the presence of barium ions.[55] The resin was filtered-off into a small column and washed thoroughly with water. Evaporation of the washings and lyophilization of the residue gave a red–brown gum. TLC analysis showed numerous components including **12** and Neu5Ac2en **3**. The majority of the product **3** was eluted from the resin with 1 to 2 M aqueous ammonia solution. Evaporation and lyophilization of the appropriate fractions

gave Neu2en **12** as an off-white hygroscopic solid. Further purification of the mixture obtained by elution with water was carried out by passage through a column of Dowex 50WX8 (H^+) (7 ml). Elution with 1.5 M aqueous ammonia solution gave **12** (overall yield 294 mg, 85%); $[\alpha]_D$ −11 (*c* 0.53, H_2O) [lit.[56] $[\alpha]_D$ −12.5 (*c* 0.50, H_2O); lit.[44] $[\alpha]_D$ −10 (*c* 0.26, H_2O)]; ^{1}H NMR δ 3.39 (1H, app.t, H-5), 3.65 (1H, dd, $J_{9,8}$ 5.7, $J_{9,9'}$ 12.0 Hz, H-9), 3.71 (1H, d, $J_{7,8}$ 9.2 Hz, H-7), 3.83 (1H, d, $J_{9',9}$ 12.0 Hz, H-9′), 3.94 (1H, m, H-8), 4.35 (1H, d, $J_{6,5}$ 10.1 Hz, H-6), 4.48 (1H, br.d, H-4), 5.65 (1H, s, H-3) [this spectrum is in agreement with that reported by Schreiner et al.[44]]; *m/z* (FAB) 272 [$(M+Na)^+$, 41%], 250 [$(M+H)^+$, 40].

4.2.2. 2,6-Anhydro-3,5-dideoxy-5-(2-hydroxyacetamido)-D-glycero-D-galacto-*non-2-enoic acid [*N*-glycolyl-Neu2en] **5***

DCC (62 mg, 0.3 mmol) was suspended in THF (3 ml) and a solution of 2-acetoxyacetic acid (32 mg, 0.3 mmol) in THF (2 ml) was added with vigorous stirring. The resulting mixture was stirred for 5 min at rt before addition to a solution of Neu2en **12** (50 mg, 0.2 mmol) in water (2 ml), triethylamine (83μl, 0.6 mmol) and THF (3 ml). Further aliquots of triethylamine were added to the reaction to maintain a pH of ca. 8 (a total of ca. 10 equiv. was often added). The reaction was monitored by TLC, and after 1 h further portions of Et_3N, DCC and 2-acetoxyacetic acid were added under the same conditions as initially used. The reaction was worked-up by addition of ca. 10 ml of water, filtration of the mixture, and evaporation of the filtrate under reduced pressure. The crude *N*-(2-acetoxyacetyl)-Neu2en was dissolved in water (3 ml), the solution treated with 0.1 M NaOH solution to pH ~9, and the reaction left at rt for 2 h. The reaction was neutralized with 1 M AcOH, concentrated and the crude *N*-(2-hydroxyacetyl)-Neu2en subject to ion-exchange chromatography. An aqueous solution of the crude product was passed through a column of Dowex 50WX8 (H^+) resin (ca. 10 ml). The *N*-acylated product was eluted with water while any unreacted **12** could be recovered by elution with 1.5–2 M aqueous ammonia solution. The fractions containing the *N*-acylated product were applied to a column of Dowex 1X8 (acetate) resin (ca. 12 ml) and elution with a gradient of acetic acid was carried out (traces of the reagent carboxylic acid remaining after this procedure could be removed by repeating the purification on the anionic resin). Elution with 4 M AcOH, followed by evaporation and repeated lyophilization gave **5** as a white solid (60 mg, 95%); $[\alpha]_D$ +21 (*c* 0.21, H_2O); ^{1}H NMR δ 3.61 (1H, d, $J_{7,8}$ 8.8 Hz, H-7), 3.64 (1H, m, H-9), 3.84 (1H, br.d, $J_{9',9}$ 12.0 Hz, H-9′), 3.89 (1H, m, H-8), 4.15 (3H, m, H-5, glycolyl CH_2), 4.35 (1H, d, $J_{6,5}$ 10.8 Hz, H-6), 4.57 (1H, d, $J_{4,5}$ 8.9 Hz, H-4), 5.99 (1H, s, H-3); ^{13}C NMR δ 52.0 (C-5), 63.7 (C-9*), 65.7 (glycolyl *C*H_2*), 69.7 (C-7†), 70.6 (C-4†), 72.6 (C-8†), 78.5 (C-6†), 115.1 (C-3), 146.5 (C-2), 168.3 (C-1), 178.2 (glycolyl *C*ONH) [*,† tentative assignments]; *m/z* 368 [$(M\cdot Na+K)^+$, 8%], 352 [$(M\cdot Na+Na)^+$, 100], 330 [$(M+Na)^+$, 50]; HRMS: calcd for $C_{11}H_{17}NO_9\cdot H$ 308.09816, found 308.09740.

4.2.3. 2,6-Anhydro-3,5-dideoxy-5-(2-chloroacetamido)-D-glycero-D-galacto-*non-2-enoic acid [*N*-chloroacetyl-Neu2en] **6***

Prepared by reaction of Neu2en **12** with DCC/chloroacetic acid as described above for the preparation of *N*-(2-acetoxyacetyl)-Neu2en in the synthesis of **5**. Elution from Dowex 1X8 (acetate) resin with 1 to 2 M AcOH, followed by evaporation and repeated lyophilization gave **6** as a white solid (90%); $[\alpha]_D$ +14.6 (*c* 0.26, H_2O) [lit.[56] $[\alpha]_D$ +33.2 (*c* 0.50, H_2O); ^{1}H NMR δ 3.73 (2H, m, H-7, H-9), 3.96 (1H, dd, $J_{9',8}$ 2.7, $J_{9',9}$ 11.3 Hz, H-9′), 4.01 (1H, ddd, $J_{8,7}$ 9.0, $J_{8,9}$ 6.3, $J_{8,9'}$ 2.7 Hz, H-8), 4.26 (1H, br.app.t, H-5), 4.29 (2H, s, ClCH_2CO), 4.48 (1H, d, $J_{6,5}$ 10.8 Hz, H-6), 4.67 (1H, dd, $J_{4,3}$ 2.4, $J_{4,5}$ 8.9 Hz, H-4), 6.14 (1H, d, $J_{3,4}$ 2.4 Hz, H-3); *m/z* 386 [$(M\cdot Na+K)^+$, 40%], 370 [$(M\cdot Na+Na)^+$, 100], 348 [$(M+Na)^+$, 37]; HRMS: calcd for $C_{11}H_{16}NO_8Cl\cdot NH_4$ 343.09082, found 343.08979.

4.2.4. 2,6-Anhydro-3,5-dideoxy-5-acrylamido-D-glycero-D-galacto-*non-2-enoic acid [*N-*(acryloyl)-Neu2en]* ***9***

To a solution of Neu2en **12** (50 mg, 0.2 mmol) in MeOH (2 ml) and Et_3N (0.5 ml) at −60°C under N_2 was added 3-chloroproprionyl chloride (58 μl, 0.6 mmol). The reaction was allowed to warm to room temperature when it was concentrated, the residue dissolved in water, and the solution subjected to ion-exchange chromatography as described above for **5**. Elution from Dowex 1X8 (acetate) resin with 2 M AcOH, followed by evaporation and repeated lyophilization gave **9** as a white solid (62%); ^{1}H NMR δ 3.61 (2H, m, H-7, H-9), 3.84 (1H, d, $J_{9',9}$ 13.2 Hz, H-9′), 3.89 (1H, m, H-8), 4.15 (1H, br.app.t, H-5), 4.31 (1H, d, $J_{6,5}$ 10.7 Hz, H-6), 4.54 (1H, d, $J_{4,5}$ 8.5 Hz, H-4), 5.78 (1H, d, *J* 8.9 Hz, olefinic-H *trans*-CONH), 5.98 (1H, s, H-3), 6.21 (1H, d, *J* 17.4 Hz, olefinic-H *cis*-CONH), 6.29 (1H, dd, *J* 8.8, *J* 17.4 Hz, olefinic-H *gem*-CONH); *m/z* 364 [(M·Na+K)$^+$, 38%], 348 [(M·Na+Na)$^+$, 100], 326 [(M+Na)$^+$, 45]; HRMS: calcd for $C_{12}H_{17}NO_8 \cdot H$ 304.10324, found 304.10283.

4.2.5. 2,6-Anhydro-3,5-dideoxy-5-(2,2,2-trichloroacetamido)-D-glycero-D-galacto-*non-2-enoic acid [*N-*trichloroacetyl-Neu2en]* ***10***

Prepared by reaction of Neu2en **12** with trichloroacetyl chloride as described above for the synthesis of **9**. Elution from Dowex 1X8 (acetate) resin with 6 M AcOH, followed by evaporation and repeated lyophilization gave **10** as a white solid (21%); ^{1}H NMR δ 3.58 (2H, m, H-7, H-9), 3.83 (1H, br.d, $J_{9',9}$ 12.2 Hz, H-9′), 3.90 (1H, m, H-8), 4.15 (1H, br.app.t, H-5), 4.41 (1H, d, $J_{6,5}$ 11.0 Hz, H-6), 4.57 (1H, d, $J_{4,5}$ 8.2 Hz, H-4), 5.88 (1H, s, H-3); *m/z* 454 [(M·Na+K)$^+$, 27%], 438 [(M·Na+Na)$^+$, 67], 416 [(M+Na)$^+$, 33]; HRMS: calcd for $C_{11}H_{14}NO_8Cl_3 \cdot NH_4$ 411.01287, found 411.01271.

4.3. Sialidase assay

Vibrio cholerae sialidase was obtained by over-expression of the *V. cholerae* nanH gene (kindly provided by Dr. E. Vimr, Illinois) in *E. coli* and subsequent purification of the enzyme as described elsewhere.[65,66] Sialidase activity was assayed using the previously reported fluorometric assay.[27] The substrate used for the enzyme assay, 2-α-(4′-methylumbelliferyl)-*N*-acetylneuraminic acid, was prepared using published methods.[67] The concentration of 2-α-(4′-methylumbelliferyl)-*N*-acetylneuraminic acid and inhibitor was varied between 50–250 μM and 5–100 μM, respectively, for the K_i determinations. Assays were performed in at least duplicate.

It should be noted that there is an almost 10-fold difference in the K_i value reported by different research groups for Neu5Ac2en against *V. cholerae* sialidase; for example, Schreiner et al.[44] 2.5×10^{-5} M, Holzer et al.[27] 3×10^{-6} M. This difference is presumably carried over into the K_i values measured for other sialic acid derivatives.[27,37] It is possible that slightly different methods of data analysis has led to this anomoly. Schreiner et al.[44] calculated constants by fitting data with a non-linear regression program to a model of partially mixed inhibition, with K_i values representing the competitive part of the model in order to facilitate comparison with older data. Holzer et al.[27] used a model of competitive inhibition. The precise effect these differences may have on inhibition data has not yet been determined. The original inhibition data for Neu5Ac2en and derivatives reported by Meindl et al. was presented either as K_i[38] or IC_{50}[39] values. Comparison of inhibition of *V. cholerae* sialidase by Neu5Ac2en derivatives has therefore been based on trends observed within sets of data.

Acknowledgements

Dr. Donald Angus is thanked for assistance with the preparation of this manuscript. We gratefully acknowledge the financial support of the Australian Research Council and GlaxoWellcome, and the Australian Government for an Australian Postgraduate Award to PF.

References

1. Schauer, R.; Kamerling, J. P. In *Glycoproteins II*; Montreuil, J.; Vliegenthart, J. F. G.; Schachter, H., Eds. Chemistry, biochemistry and biology of sialic acids. Elsevier Science: Amsterdam, 1997; pp. 243–402.
2. *Biology of the Sialic Acids*; Rosenberg, A., Ed.; Plenum Press: New York, 1995.
3. Reuter, G.; Gabius, H.-J. *Biol. Chem. Hoppe-Seyler* **1996**, *377*, 325–342.
4. Varki, A. *FASEB J.* **1997**, 248–255.
5. Izard, T.; Lawrence, M. C.; Malby, R. L.; Lilley, G. G.; Colman, P. M. *Structure* **1994**, *2*, 361–369.
6. Taylor, G. *Curr. Opin. Struct. Biol.* **1996**, *6*, 830–837.
7. Saito, M.; Yu, R. K. In *Biology of the Sialic Acids*; Rosenberg, A., Ed. Biochemistry and function of sialidases. Plenum Press: New York, 1995; pp. 261–313 and references cited therein.
8. Colman, P. M. *Protein Sci.* **1994**, *3*, 1687–1696 and references cited therein.
9. Varghese, J. N.; Laver, W. G.; Colman, P. M. *Nature* **1983**, *303*, 35–40.
10. Varghese, J. N.; Colman, P. M. *J. Mol. Biol.* **1991**, *221*, 473–486.
11. Varghese, J. N.; McKimm-Breschkin, J. L.; Caldwell, J. B.; Kortt, A. A.; Colman, P. M. *Proteins: Struct., Funct., Genet.* **1992**, *14*, 327–332.
12. Varghese, J. N.; Epa, V. C.; Colman, P. M. *Protein Sci.* **1995**, *4*, 1081–1087.
13. Burmeister, W. P.; Ruigrok, R. W. H.; Cusack, S. *EMBO J.* **1992**, *11*, 49–56.
14. Burmeister, W. P.; Henrissat, B.; Bosso, C.; Cusack. S.; Ruigrok, R. W. H. *Structure* **1993**, *1*, 19–26.
15. Crennell, S. J.; Garman, E. F.; Laver, W. G.; Vimr, E. R.; Taylor, G. L. *Proc. Natl. Acad. Sci. USA* **1993**, *90*, 9852–9856.
16. Crennell, S. J.; Garman, E. F.; Philippon, C.; Vasella, A.; Laver, W. G.; Vimr, E. R.; Taylor, G. L. *J. Mol. Biol.* **1996**, *259*, 264–280.
17. Crennell, S.; Garman, E.; Laver, G.; Vimr, E.; Taylor, G. *Structure* **1994**, *2*, 535–544.
18. Gaskell, A.; Crennell, S.; Taylor, G. *Structure* **1995**, *3*, 1197–1205.
19. Luo, Y.; Li, S.-C.; Chou, M.-Y.; Li, Y.-T.; Luo, M. *Structure* **1998**, *6*, 521–530.
20. Luo, Y.; Li, S.-C.; Li, Y.-T.; Luo, M. *J. Mol. Biol*. **1999**, *285*, 323–332.
21. White, C. L.; Janakiraman, M. N.; Laver, W. G.; Philippon, C.; Vasella, A.; Air, G. M.; Luo, M. *J. Mol. Biol.* **1995**, *245*, 623–634.
22. Watowich, S. J.; Skehel, J. J.; Wiley, D. C. *Structure* **1994**, *2*, 719–731 and references cited therein.
23. Graves, B. J.; Crowther, R. L.; Chandran, C.; Rumberger, J. M.; Li, S.; Huang, K.-S.; Presky, D. H.; Familletti, P. C.; Wolitzky, B. A.; Burns, D. K. *Nature* **1994**, *367*, 532–538.
24. von Itzstein, M.; Dyason, J. C.; Oliver, S. W.; White, H. F.; Wu, W.-Y.; Kok, G. B.; Pegg, M. S. *J. Med. Chem.* **1996**, *39*, 388–391.
25. von Itzstein, M.; Wu, W.-Y.; Kok, G. B.; Pegg, M. S.; Dyason, J. C.; Jin, B.; Phan, T. V.; Smythe, M. L.; White, H. F.; Oliver, S. W.; Colman, P. M.; Varghese, J. N.; Ryan, D. M.; Woods, J. M.; Bethell, R. C.; Hotham, V. J.; Cameron, J. M.; Penn, C. R. *Nature* **1993**, *363*, 418–423.
26. von Itzstein, M.; Wu, W.-Y.; Jin, B. *Carbohydr. Res.* **1994**, *259*, 301–305.
27. Holzer, C. T.; von Itzstein, M.; Jin, B.; Pegg, M. S.; Stewart, W. P.; Wu, W.-Y. *Glycoconjugate J.* **1993**, *10*, 40–44.
28. Chandler, M.; Bamford, M. J.; Conroy, R.; Lamont, B.; Patel, B.; Patel, V. K.; Steeples, I. P.; Storer, R.; Weir, N. G.; Wright, M.; Williamson, C. *J. Chem. Soc., Perkin Trans. 1* **1995**, 1173–1180.
29. Kiefel, M. J.; von Itzstein, M. *Prog. Med. Chem.* **1999**, *36*, 1–28.
30. Calfee, D. P.; Hayden, F. G. *Drugs* **1998**, *56*, 537–553.
31. Waghorn, S. L.; Goa, K. L. *Drugs* **1998**, *55*, 721–725.
32. Stewart-Tull, D. E. S.; Ollar, R. A.; Scobie, T. S. *J. Med. Microbiol.* **1986**, *22*, 325–333.
33. Galen, J. E.; Ketley, J. M.; Fasano, A.; Richardson, S. H.; Wasserman, S. S.; Kaper, J. B. *Infect. Immun.* **1992**, *60*, 406–415 and references cited therein.

34. Merritt, E. A.; Sarfaty, S.; van den Akker, F.; L'Hoir, C.; Martial, J. A.; Hol, W. G. J. *Protein Sci.* **1994**, *3*, 166–175 and references cited therein.
35. Holmquist, L. *FOA Reports* **1975**, *9*, 1–20.
36. Corfield, A. P.; Schauer, R. In *Sialic Acids — Chemistry, Metabolism and Function*; Schauer, R., Ed. Metabolism of sialic acids. Springer: Wien, 1982; pp. 195–261.
37. Zbiral, E. In *Carbohydrates — Synthetic Methods and Applications in Medicinal Chemistry*; Ogura, H.; Hasegawa, A.; Suami, T., Eds. Synthesis of sialic acid analogs and their behavior towards the enzymes of sialic acid metabolism and hemagglutinin X-31 of influenza A-virus. VCH: Weinheim, 1992; pp. 304–339.
38. Meindl, P.; Tuppy, H. *Hoppe-Seyler's Z. Physiol. Chem.* **1969**, *350*, 1088–1092.
39. Meindl, P.; Bodo, G.; Palese, P.; Schulman, J.; Tuppy, H. *Virology* **1974**, *58*, 457–463.
40. Khorlin, A. Ya.; Privalova, I. M.; Zakstelskaya, L. Ya.; Molibog, E. V.; Evstigneeva, N. A. *FEBS Lett.* **1970**, *8*, 17–19.
41. Brossmer, R.; Bürk, G.; Eschenfelder, V.; Holmquist, L.; Jäckh, R.; Neumann, B.; Rose, U. *Behring Inst. Mitt.* **1974**, *55*, 119–123.
42. Brossmer, R.; Keilich, G.; Ziegler, D. *Hoppe-Seyler's Z. Physiol. Chem.* **1977**, *358*, 391–396.
43. Nöhle, U.; Shukla, A. K.; Schröder, C.; Reuter, G.; Schauer, R.; Kamerling, J. P.; Vliegenthart, J. F. G. *Eur. J. Biochem.* **1985**, *152*, 459–463.
44. Schreiner, E.; Zbiral, E.; Kleineidam, R. G.; Schauer, R. *Carbohydr. Res.* **1991**, *216*, 61–66.
45. Schreiner, E.; Zbiral, E. *Liebigs Ann. Chem.* **1990**, 581–586 and references cited therein.
46. Miller, C. A.; Wang, P.; Flashner, M. *Biochem. Biophys. Res. Commun.* **1978**, *83*, 1479–1487.
47. Furuhata, K.; Sato, S.; Goto, M.; Takayanagi, H.; Ogura, H. *Chem. Pharm. Bull.* **1988**, *36*, 1872–1876.
48. Chong, A. K. J.; Pegg, M. S.; Taylor, N. R.; von Itzstein, M. *Eur. J. Biochem.* **1992**, *207*, 335–343.
49. Taylor, N. R.; von Itzstein, M. *J. Med. Chem.* **1994**, *37*, 616–624.
50. Goodford, P. J. *J. Med. Chem.* **1985**, *28*, 849–857.
51. Vasella, A.; Wyler, R. *Helv. Chim. Acta* **1991**, *74*, 451–463.
52. Vasella, A.; Wyler, R. *Helv. Chim. Acta* **1990**, *73*, 1742–1763.
53. Lentz, M. R.; Webster, R. G.; Air, G. M. *Biochemistry* **1987**, *26*, 5351–5358.
54. Okamoto, K.; Kondo, T.; Goto, T. *Bull. Chem. Soc. Jpn.* **1987**, *60*, 631–636.
55. Isecke, R.; Brossmer, R. *Tetrahedron* **1994**, *50*, 7445–7460.
56. Meindl, P.; Tuppy, H. *Monatsh. Chem.* **1973**, *104*, 402–414.
57. Smith, P. W.; Starkey, I. D.; Howes, P. D.; Sollis, S. L.; Keeling, S. P.; Cherry, P. C.; von Itzstein, M.; Wu, W.-Y.; Jin, B. *Eur. J. Med. Chem.* **1996**, *31*, 143–150.
58. Roy, R.; Laferrière, C. A. *Can. J. Chem.* **1990**, *68*, 2045–2054.
59. Brossmer, R.; Gross, H. J. *Methods Enzymol.* **1994**, *247*, 153–176.
60. Sparks, M. A.; Williams, K. W.; Lukacs, C.; Schrell, A.; Priebe, G.; Spaltenstein, A.; Whitesides, G. M. *Tetrahedron* **1993**, *49*, 1–12.
61. Sugata, T.; Kan, Y.; Nagaregawa, Y.; Miyamoto, T.; Higuchi, R. *J. Carbohydr. Chem*. **1997**, *16*, 917–925.
62. Choi, S.-K.; Lee, S.; Whitesides, G. M. *J. Org. Chem.* **1996**, *61*, 8739–8745.
63. Taylor, N. R.; von Itzstein, M. *J. Comput.-Aided Mol. Des.* **1996**, *10*, 236–246.
64. Anschütz, R.; Bertram, W. *Ber.* **1903**, *36*, 466–468.
65. Vimr, E. R.; Lawrisuk, L.; Galen, J.; Kaper, J. B. *J. Bacteriol*. **1988**, *170*, 1495–1504.
66. Taylor, G.; Vimr, E.; Garman, E.; Laver, G. *J. Mol. Biol.* **1992**, *226*, 1287–1290.
67. Myers, R. W.; Lee, R. T.; Lee, Y. C.; Thomas, G. H.; Reynolds, L. W.; Uchida, Y. *Anal. Biochem.* **1980**, *101*, 166–174.